PHYSICAL REVIEW A, VOLUME 64, 022709

Accurate amplitudes for electron-impact ionization

M. Baertschy
JILA, University of Colorado, UCB 440, Boulder, Colorado 80309-0440

T. N. Rescigno
Computing Sciences, Lawrence Berkeley National Laboratory, Berkeley, California 94720
and Physics Directorate, Lawrence Livermore National Laboratory, Livermore, California 94551

C. W. McCurdy
Computing Sciences, Lawrence Berkeley National Laboratory, Berkeley, California 94720
and Department of Applied Science, University of California, Davis, Livermore, California 94551
(Received 14 March 2001; published 9 July 2001)

We show that the ‘‘two-potential’’ formalism of conventional distorted-wave rearrangement theory, which is formally valid only for short-range interactions, can be used to evaluate amplitudes for the ionization of atomic hydrogen by electron impact. The triply differential cross sections calculated using this method validate earlier results obtained by extrapolating the quantum mechanical flux. Although it uses the same time-independent wave functions, this method offers significant advantages over flux extrapolation. It is more accurate, can be applied in practical calculations over a broader range of collision energies, and unlike the flux-extrapolation method, can be applied for arbitrary values of energy sharing between the ejected electrons. Since this rearrangement formalism provides the complete scattering amplitude for ionization, it can be used to calculate any differential cross section.

DOI: 10.1103/PhysRevA.64.022709 PACS number(s): 34.80.Dp

I. INTRODUCTION

Ionization of atomic hydrogen by electron impact is one of the simplest examples of a three-body Coulomb problem. It is one which has continued to attract the attention of theorists since the 1960s when the quantum mechanical formulation was first outlined by Peterkop [1] and by Rudge and Seaton [2,3]. Most of the computational studies carried out have been based on perturbation theory, which becomes increasingly unreliable as the collision energy decreases. While various nonperturbative approaches have been developed and shown capable of producing accurate total ionization cross sections, only recently has a complete and accurate quantum mechanical solution appeared feasible. The development of accurate *ab initio* methods that can be applied with reliability at energies of a few electron volts or less above the ionization energy will be crucial in probing the dynamics of threshold ionization, since most of our present understanding of that difficult region is based on classical and semiclassical theory [4].

In a series of papers [5–9] we developed a procedure for solving the time-independent Schrödinger equation for the wave function describing electron-hydrogen scattering above the ionization threshold and from that produced various differential cross sections describing the dynamics of the two outgoing electrons following ionization. Our basic approach to the electron-impact ionization problem consists of two distinct steps. First, we calculate the outgoing wave portion of the full scattering wave function on a finite volume. By using an exterior complex scaling transformation of the electronic coordinates, this can be accomplished without recourse to any explicit asymptotic form for the scattered wave.

The second step consists of using the calculated scattered waves to extract detailed dynamical information about ionization. In the work referenced above, the extraction procedure we used was also designed to avoid relying on asymptotic boundary conditions. This was accomplished by directly evaluating the quantum mechanical flux through a finite (hyper) surface that bounds the region where we know the wave function followed by a numerical extrapolation to infinite volume, where the flux can be related to the differential cross sections for ionization. In two-dimensional model problems the cross sections computed this way could be made arbitrarily accurate [10]. When applied to the full problem of electron-hydrogen scattering [7,8] this approach produced triply differential cross sections (TDCS) at equal energy sharing that agree remarkably well with experiment [11,12] and singly differential cross sections (SDCS) that exhibited the low-energy behavior predicted by earlier semiclassical work [13].

Despite its successes, the flux-extrapolation method has its limitations. Even for collisions with only short-range interactions, evaluating the asymptotic flux can require calculations well beyond the range of the potentials, since it is tied to the asymptotic behavior of the scattering wave function. For example, the asymptotic form of the full wave function for simple potential scattering,

$$\Psi^{+}(\mathbf{r}) \xrightarrow[r\to\infty]{} e^{i\mathbf{k}\cdot\mathbf{r}}+e^{ikr}[f(\theta)/r+O(1/r^{2})], \qquad (1.1)$$

has corrections of order $1/r^2$, even for finite-range potentials. This fact is rarely emphasized in textbook introductions to scattering theory, since it is irrelevant to the common integral expressions for the scattering amplitude, $f(\theta)$, but it is quite relevant in determining the asymptotic flux. There are additional complications with the flux-extrapolation method in the case of Coulomb interactions. The method requires the use of grids large enough to allow the physical region inhabited only by the ionization portion of the scattered wave to be distinguishable from the parts that describe discrete two-body channels. The requirement that the ionization wave be "uncovered" before the asymptotic flux is calculated can require grids that extend well beyond the range where the interaction potentials are appreciable and sets practical lower limits on the collision energies that can be considered. The flux-extrapolation procedure is inherently limited in its ability to describe ionization when a single electron carries most of the available energy. This is due to its inability to distinguish between excitation channels and ionization where energy is shared asymmetrically. Consequently, in our previous work we were able to calculate *ab initio* SDCS's only when one electron carried no more than about 75% of the total energy [14]. Similarly, triply and doubly differential cross sections [9] were calculated most reliably at or near equal energy sharing. Even in the regime where the calculation was deemed reliable, comparison to the assumed asymptotic form implies error on the order of 10% [14]. In principle, these limitations could be made arbitrarily small by increasing the size of the calculation, but in practice the method falls short of being truly complete.

In this paper we report on a procedure for extracting ionization cross sections from the computed scattered wave function that offers significant improvements over the flux-extrapolation method. We show results for singly and triply differential cross sections obtained from ionization *amplitudes* that are calculated using a "two-potential" formalism derived from conventional distorted-wave rearrangement theory. The technique was initially developed in the context of short-range interactions and applied to several two-dimensional model problems [15]. The formalism was then extended to include the case of Coulomb interactions [16] and we have recently demonstrated that we could use the method to calculate the *S*-wave component of the SDCS for the full *e*-H scattering problem [17]. Since the SDCS is an incoherent sum of partial-wave contributions, its evaluation does not require phase coherence between various partial-wave components of the ionization amplitude. Previously, we expressed concern that a method which is formally valid only for short-range interactions might lead to phase inconsistencies when applied to a partial-wave expansion of the scattered wave [16] in the case of Coulomb interactions. This would have made calculating the doubly and triply differential ionization cross sections with this formalism impossible. In this paper we report that no such difficulty exists and we will show that the rearrangement formalism can be used to accurately calculate differential ionization cross sections free from the limitations inherent in the flux-extrapolation method.

II. THEORY

The cross sections presented here were extracted from wave functions calculated in exactly the same manner as in our previous work. The first step in our approach is to solve the time-independent Schrödinger equation for electron-hydrogen scattering using the method of exterior complex scaling to simplify the scattering boundary conditions. We partition the total wave function Ψ^+ into an appropriately symmetrized unperturbed state $\Psi^0_{k_i}$, describing a free electron with momentum $\mathbf{k}_i$ incident on a ground-state hydrogen atom:

$$\Psi^0_{k_i} = \frac{1}{\sqrt{2}} [\Phi_{1s}(\mathbf{r}_1) e^{i\mathbf{k}_i \cdot r_2} + (-1)^s \Phi_{1s}(\mathbf{r}_2) e^{i\mathbf{k}_i \cdot \mathbf{r}_1}], \tag{2.1}$$

and a scattered wave term Ψ^+_{sc}. The wave functions are either symmetric (for total spin $S=0$) or antisymmetric ($S=1$) with respect to interchange of the two electronic coordinates. The scattered wave function Ψ^+_{sc} is defined as the outgoing solution of the inhomogeneous differential equation

$$(E-H)\Psi^+_{\mathrm{sc}}(\mathbf{r}_1,\mathbf{r}_2) = (H-E)\Psi^0_{k_i}(\mathbf{r}_1,\mathbf{r}_2), \tag{2.2}$$

which comes from rearrangement of the Schrödinger equation. Details of how we solve Eq. (2.2) can be found elsewhere [8] and will be described only briefly here.

The scattered wave function Ψ^+_{sc} is expanded in terms of coupled spherical harmonics $\mathcal{Y}^{L0}_{l_1,l_2}(\hat{r}_1,\hat{r}_2)$:

$$\Psi^+_{\mathrm{sc}}(\mathbf{r}_1,\mathbf{r}_2) = \sum_{L,l_1,l_2} \frac{i^L}{r_1 r_2} \psi^L_{l_1,l_2}(r_1,r_2) \mathcal{Y}^{L0}_{l_1,l_2}(\hat{r}_1,\hat{r}_2). \tag{2.3}$$

Each of the radial functions $\psi^L_{l_1 l_2}(r_1,r_2)$ has outgoing-wave boundary conditions. In order to calculate the $\psi^L_{l_1 l_2}$ we use the method of exterior complex scaling (ECS) where all radial coordinates are mapped to a contour,

$$r \rightarrow \begin{cases} r, & r < R_0, \\ R_0 + (r-R_0)e^{i\eta}, & r \geqslant R_0, \end{cases} \tag{2.4}$$

that is real for $r \leqslant R_0$, but rotated into the upper half of the complex plane beyond R_0. Any outgoing wave evaluated on this contour becomes exponentially damped beyond R_0. Under the ECS transformation the $\psi^L_{l_1 l_2}$ are square integrable functions that we calculate directly on a two-dimensional radial grid by solving sets of coupled, two-dimensional, complex differential equations for each value of L and S.

The rearrangement formalism we use for calculating the ionization amplitude was developed in two previous papers [15,16] within the context of two-dimensional models of electron-hydrogen scattering. It is similar to the formalism given by Whelan *et al.* [18] and is used as the starting point for a number of "ansatz" approximations discussed by Lucey, Rasch, and Whelan [19]. Here we will present a straightforward generalization of the formalism to the six-dimensional, two-electron problem.

In Ref. [16], we showed that if we started with an expression for the ionization amplitude, $\mathcal{F}(k_1,k_2)$, that is, a function of the momentum vectors for both outgoing electrons,

$$\mathcal{F}(k_1,k_2)=\langle \phi^0_{k_1}\phi^0_{k_2}|V|\Psi^+\rangle, \tag{2.5}$$

in terms of undistorted plane waves,

$$\phi^0_k(r)=e^{ik\cdot r}, \tag{2.6}$$

then we could use conventional rearrangement theory to derive an equivalent volume integral expression in terms of Coulomb distorted waves:

$$\mathcal{F}(\mathbf{k}_1,\mathbf{k}_2)=\langle \Phi^{(-)}_{\mathbf{k}_1}\Phi^{(-)}_{\mathbf{k}_2}|E-T-V_1|\Psi^+_{\mathrm{sc}}\rangle. \tag{2.7}$$

In Eq. (2.7), E is the total energy, T is the two-electron kinetic energy operator, V_1 is the sum of all one-electron potentials defined as

$$V_1(\mathbf{r}_1,\mathbf{r}_2)\equiv-\frac{1}{r_1}-\frac{1}{r_2}, \tag{2.8}$$

and the $\Phi^{(-)}_{\mathbf{k}}(\mathbf{r})$ are Coulomb functions with effective charge 1, momentum $\mathbf{k}$, and incoming-wave boundary conditions. The integral in Eq. (2.7) must be evaluated over a finite volume that lies within a region where both electronic coordinates are real. We generally choose this to be the volume enclosed by a hyperradius $\rho\equiv\sqrt{(r_1^2+r_2^2)}\leqslant R_0$. Equation (2.7) has an equivalent surface integral representation which appears upon application of Green's theorem and is more convenient for numerical calculations:

$$\mathcal{F}(\mathbf{r}_1,\mathbf{k}_2)=\tfrac{1}{2}\int_S(\Phi^{(+)}_{\mathbf{k}_1}\Phi^{(+)}_{\mathbf{k}_2}\boldsymbol{\nabla}\Psi^+_{\mathrm{sc}}-\Psi^+_{\mathrm{sc}}\boldsymbol{\nabla}\Phi^{(+)}_{\mathbf{k}_1}\Phi^{(+)}_{\mathbf{k}_2})\cdot d\hat{\mathbf{S}}. \tag{2.9}$$

The formal theory of ionization [1–3] shows that there is a phase factor associated with the integral in Eq. (2.9) that diverges as the enclosed volume becomes infinite. To eliminate the divergence of the phase, the formal theory requires that the Coulomb functions carry effective charges z_1 and z_2 that satisfy the so-called Peterkop relation [20]

$$\frac{z_1}{k_1}+\frac{z_2}{k_2}=\frac{1}{k_1}+\frac{1}{k_2}-\frac{1}{|\mathbf{k}_1-\mathbf{k}_2|}. \tag{2.10}$$

If we were to impose this condition in choosing the Coulomb distorted waves, however, they would no longer be orthogonal to the hydrogenic bound states and, as shown in Ref. [16], this orthogonality is essential in eliminating the contributions from one-electron terms that formally vanish on an infinite volume but would otherwise "contaminate" the calculated $\mathcal{F}$ when the integration in Eq. (2.7) is over a finite volume. For this reason, it is important that the $\Phi^{(-)}_{\mathbf{k}}$ be associated with charge one rather than effective charges that satisfy the Peterkop relation. We will see below that failure to enforce the Peterkop relation does not lead to any phase ambiguities, provided that the ionization amplitudes are evaluated appropriately.

To evaluate Eq. (2.9) with the partial-wave expansion of Ψ^+_{sc} in Eq. (2.3) we use the expansion of $\Phi^{(-)}_{\mathbf{k}}$ in spherical harmonics:

$$\Phi^{(-)}_{\mathbf{k}}(\mathbf{r})=\sum_{l=0}^{\infty}\sum_{m=-l}^{l}\frac{i^l e^{-i\eta_l}}{\sqrt{kr}}\hat{\phi}_l(k;r)Y^{\star}_{l,m}(\hat{\mathbf{k}})Y_{l,m}(\hat{\mathbf{r}}), \tag{2.11}$$

where $\eta_l\equiv\arg\{\Gamma(l+1-i/k)\}$ and the $\hat{\phi}_l$ are regular solutions of the radial Coulomb equation

$$\left[-\frac{1}{2}\frac{d^2}{dr^2}+\frac{l(l+1)}{2r^2}-\frac{1}{r}\right]\hat{\phi}_l(k;r)=\frac{k^2}{2}\hat{\phi}_l(k;r). \tag{2.12}$$

After substituting the expansions in Eqs. (2.3) and (2.11) into Eq. (2.9) and integrating over the angular coordinates $\hat{\mathbf{r}}_1$ and $\hat{\mathbf{r}}_2$ we arrive at a partial-wave expansion of the ionization amplitude in Eq. (2.7):

$$\mathcal{F}(k_1,k_2)=\sum_{L,l_1,l_2}i^{L-l_1-l_2}e^{i(\eta_{l_1}+\eta_{l_2})}f^L_{l_1l_2}(k_1,k_2)\mathcal{Y}^{L0}_{l_1,l_2}(\mathbf{k}_1,\mathbf{k}_2). \tag{2.13}$$

The partial-wave amplitudes $f^L_{l_1l_2}$ in Eq. (2.13) are defined by expressions analogous to Eq. (2.9). If we use hyperspherical coordinates ρ and α such that $r_1=\rho\cos\alpha$ and $r_2=\rho\sin\alpha$, then the explicit expression for the $f^L_{l_1l_2}$ is a one-dimensional surface integral evaluated at some hyperradius $\rho=\rho_0$:

$$\begin{aligned}f^L_{l_1l_2}(k_1,k_2;\rho_0)&=\frac{\rho_0}{2\sqrt{k_1k_2}}\int_0^{\pi/2}\left[\hat{\phi}_{l_1}(k_1,r_1)\hat{\phi}_{l_2}(k_2,r_2)\frac{d}{d\rho}\psi^L_{l_1l_2}\right.\\&\left.\left.\quad-\psi^L_{l_1l_2}\frac{d}{d\rho}[\hat{\phi}_{l_1}(k_1,r_1)\hat{\phi}_{l_2}(k_2,r_2)]\right]\right|_{\rho=\rho_0}d\alpha.\end{aligned} \tag{2.14}$$

Equation (2.14) is used to calculate the $f^L_{l_1l_2}$ for each partial-wave radial function $\psi^L_{l_1l_2}$. The complete ionization amplitude can then be constructed according to Eq. (2.13) and from that any differential cross section for ionization can be calculated.

III. CALCULATION

Calculating the scattered wave is by far the most computationally intensive of the two steps in our approach. Because of the number of terms kept in the partial-wave expansion and the size of the two-dimensional radial grid required, we need to solve linear systems of a few 10^6 complex equations. The techniques used to calculate Ψ^+_{sc} have been described in detail elsewhere [8]. The complex scaling point R_0 used ranges from $80a_0$ at the highest energy considered to $130a_0$

at the lowest energy. Within a box of length R_0 the radial coordinates are real and the calculated $\psi^L_{l_1 l_2}$ are equal to those of the physical (unscaled) scattered wave. The calculated $\psi^L_{l_1 l_2}$ are usable only within this box, so the hyperradius ρ_0 of the surface used to evaluate the $f^L_{l_1 l_2}$ in Eq. (2.14) is constrained by $\rho_0 \leqslant R_0$.

To calculate the $f^L_{l_1 l_2}$ we numerically integrate along a quarter-circle of radius ρ_0 in the r_1, r_2 plane. We use Gauss-Legendre quadrature to evaluate the integrals. The integrand in Eq. (2.14) can be highly oscillatory, so care must be taken to ensure that sufficient quadrature points are used. We calculate the $f^L_{l_1 l_2}$ for each partial wave over a range of k_1 with k_2 constrained by energy conservation, $k_2^2 = 2E - k_1^2$. We also calculated the $f^L_{l_1 l_2}$ for a range of ρ_0. Once we have calculated all of the $f^L_{l_1 l_2}$ we can reconstruct the ionization amplitude, $\mathcal{F}$, according to Eq. (2.13). The TDCS, which is differential in energy sharing and the directions of both outgoing electrons, is obtained directly from $\mathcal{F}$ by the simple expression

$$\sigma_{\text{ion}}(\mathbf{k}_1 \mathbf{k}_2) = \frac{16\pi^2}{k_i^2} |\mathcal{F}(\mathbf{k}_1 \mathbf{k}_2)|^2. \tag{3.1}$$

We have mentioned the fact that there is a ρ_0-dependent phase associated with Eq. (2.9) that diverges in the limit $\rho_0 \to \infty$. Since the enclosed integration volume is finite, the phase does not diverge and a single volume-dependent phase that multiplies the full ionization amplitude will make no contribution to any computed cross section. To produce a TDCS by reconstructing the full ionization amplitude from partial-wave components it is essential that all of the $f^L_{l_1 l_2}$ come from integration along arcs of the same hyperradius ρ_0. Using $f^L_{l_1 l_2}$ evaluated at different ρ_0 would, undoubtedly, create problems due to phase inconsistencies among the individual terms in Eq. (2.13). We previously expressed some concern [16] that numerical instabilities in the phase might, in practice, lead to inconsistencies among the partial-wave terms, even though the phases of the $f^L_{l_1 l_2}$ are formally consistent if they are all calculated at the same ρ_0. We have found that there is no phase inconsistency, as evidenced by the TDCS results presented in the next section.

The other differential cross section that we will consider in this paper is the SDCS which is differential with respect to the energy of one of the outgoing electrons. The SDCS is obtained from the TDCS by integrating over the angular coordinates of both momenta $\mathbf{k}_1$ and $\mathbf{k}_2$. Because of orthonormality of the $\mathcal{Y}^{L0}_{l_1, l_2}$ in Eq. (2.13), the SDCS can be expressed as a simple sum of individual partial-wave terms

$$\sigma_{\text{ion}}(k_1, k_2) = \frac{16\pi^2}{k_i^2} \sum_{L, l_1, l_2} |f^L_{l_1 l_2}(k_1, k_2)|^2. \tag{3.2}$$

It is worth noting that, according to Eq. (3.2), the SDCS would be impervious to any phase inconsistencies, if they existed, among the $f^L_{l_1 l_2}$. The cross section definitions given in Eqs. (3.1) and (3.2) are normalized so that the total ionization cross section is given by integrating the SDCS over half of the total energy:

$$\sigma_{\text{ion}}(E) = \int_0^{E/2} \sigma_{\text{ion}}(\sqrt{2\epsilon}, \sqrt{2(E-\epsilon)}) d\epsilon. \tag{3.3}$$

By manipulating Eq. (2.7) and using Eq. (2.2), it is easy to show that the ionization amplitude can be written as

$$\mathcal{F}(\mathbf{k}_1, \mathbf{k}_2) = \langle \Phi^{(-)}_{\mathbf{k}_1} \Phi^{(-)}_{\mathbf{k}_2} | V_{12} | \Psi^+ \rangle, \tag{3.4}$$

which shows that it formally requires integration over the range of the two-body part of the interaction potential. Since the electron-electron repulsion is of infinite range, it is natural to enquire about the dependence of the cross sections on the size and shape of the volumes enclosed in computing the amplitudes. We have made the empirical observation that the volume integral in Eq. (2.7) should always be over a hypersphere. We found that evaluating the $f^L_{l_1 l_2}$ by integrating over other closed surfaces—for example, over a hypercube defined by r_1, $r_2 \leqslant R_0$—produced spurious oscillations in the SDCS on the order of several percent, which diminish as R_0 is increased. When we look at the dependence of cross sections upon the hyperradius at which the underlying amplitudes were calculated, we observe small amplitude oscillations generally on the order of a few percent. It is possible that further investigation will shed light on the origin of these oscillations and suggest ways of minimizing the associated errors. For now, we use the observed dependence of the cross sections upon ρ_0 to estimate the accuracy of the results presented in the next section.

IV. RESULTS

In an earlier paper [8] we reported singly and triply differential cross sections, derived from flux extrapolation, for collision energies of 17.6, 19.6, 25, and 30 eV. We have since recalculated those cross sections using the procedure described in the previous section. A representative sample of the results are reported here. We wish to stress that the results at these energies were extracted from the same $\psi^L_{l_1 l_2}$ that were calculated in our earlier work. Thus, we have two independent means of calculating differential cross sections from the same numerical wave function.

The first results we report are for the SDCS as calculated using Eq. (3.2). These are shown, along with the individual singlet and triplet components, in Fig. 1. With the SDCS there is no concern over possible phase inconsistencies among the different $f^L_{l_1 l_2}$. Based on our earlier work using this rearrangement formalism [15–17], we can be certain of the accuracy of the magnitudes of the $f^L_{l_1 l_2}$. For the four collision energies covered in Ref. [8] we also show the SDCS derived from flux extrapolation. Agreement in shape between results from the two methods is very good and confirms the flattening of the SDCS with decreasing energy predicted by semiclassical theory [13].

Primarily, the disagreement between the SDCS calculated

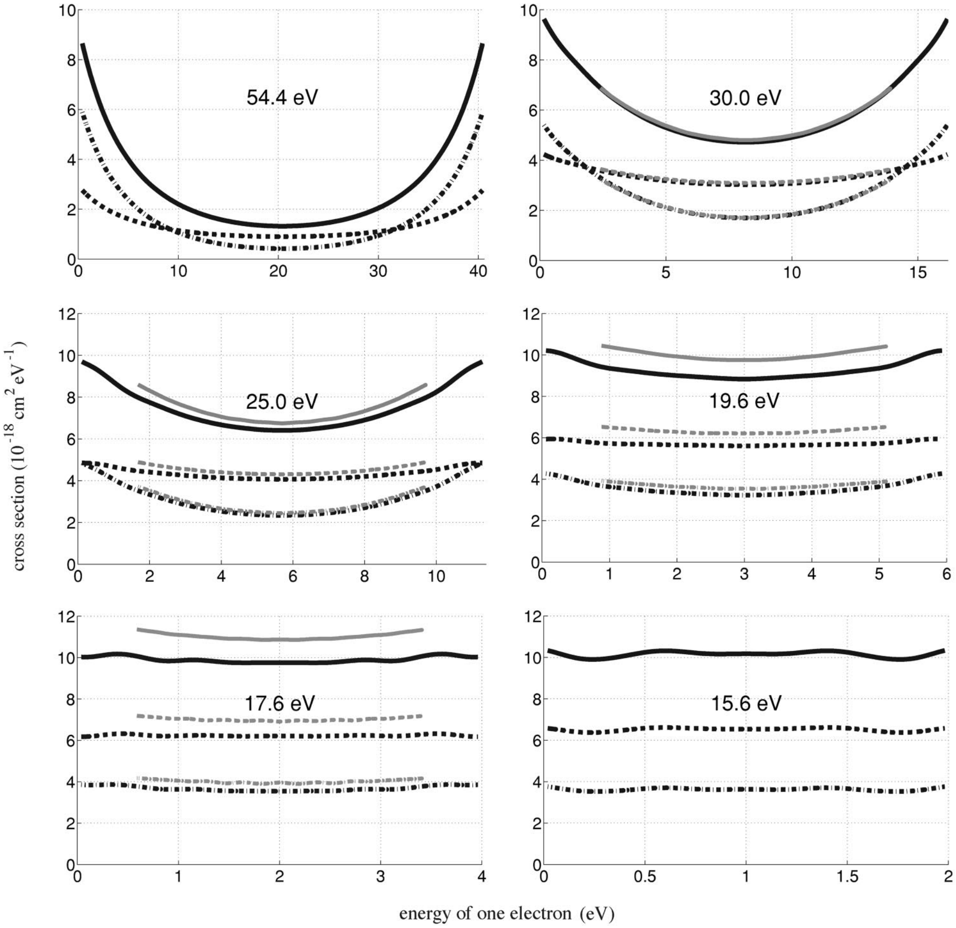

FIG. 1. Singly differential cross sections for e-H scattering at the collision energies indicated. Individual components for singlet (dashed line) and triplet (dot-dashed line) are shown. Where applicable, earlier results based on flux extrapolation [8] are shown in light gray.

using Eq. (3.2) and the SDCS derived from flux extrapolation is in the overall magnitude rather than the shape. Flux extrapolation seems to produce SDCS results that are systematically too high. The difference diminishes with increasing energy from about 10% at 17.6 eV to less than 2% by 30 eV. However, even at the lower collision energies the disagreement is not beyond what one would expect after closely examining the flux-extrapolation procedure [14]. As stated earlier, we found that the SDCS calculated from Eq. (3.2) exhibits small amplitude oscillations, as a function of the hyperradius ρ_0 at which the underlying $f^L_{l_1 l_2}$ were calculated. The origin of these small oscillations, which diminish with increasing ρ_0, is not yet fully understood, but we hasten to add that there is no *a priori* reason why convergence of the SDCS with increasing box size be exactly monotonic. For now, we obtain our final results by averaging through these oscillations. Using the amplitude of the oscillations as an indicator of the accuracy of the calculation we estimate that the SDCS are accurate to within 5% for 17.6 eV and 2% for 30 eV.

In Fig. 1 we show the SDCS for 15.6 eV collision energy, just 2 eV above threshold. At this low energy we were unable to obtain reliable results using flux extrapolation. Even the $f^L_{l_1 l_2}$ exhibit a more pronounced dependence upon ρ_0 than those calculated at the other energies, with the expected uncertainty of our SDCS being higher at this energy. At 15.6 eV the SDCS is found to have the same flattened shape first noticed at 17.6 eV. At both of these energies, the procedure has revealed subtle transitions in the SDCS from the simpler bow-shaped curves seen at the higher energies. These structures could not be found by the older flux-extrapolation method because flux extrapolation was unable to produce the SDCS over the full range of energy sharing, as indicated in Fig. 1. The orthogonality of the Coulomb distorted waves to the bound hydrogenic functions makes the ionization amplitudes computed using Eq. (2.14) free from any ‘‘contamination’’ by two-body channels contained in the scattered wave and we are now able to calculate the SDCS over the full range of energy sharing.

We also show results for the SDCS at 54.4 eV collision energy. At this relatively high energy the ρ_0 dependence in Eq. (2.14) is very small, so the $f^L_{l_1 l_2}$ should be very accurate. However, convergence of the angular momentum expansion requires more partial-wave terms at this energy than we were able to include. This limits the accuracy of the 54.4 eV SDCS shown in Fig. 1 which we present here primarily to illustrate the dependence of the shape of the SDCS upon the total energy. Our *ab initio* calculation included angular momentum components up to $L = 13$. Beyond $L = 4$ the individual L components decay exponentially with increasing L. We estimated the contributions from $L > 13$ by assuming a simple exponential decay law for large L. The effect of the large-L components that were estimated is to raise the SDCS by about 7% near the wings of the distribution.

TABLE I. Singlet, triplet, and total ionization cross sections and the spin asymmetry. Cross sections are in units of a_0^2; asymmetry is dimensionless. Spin factors are not included in the singlet and triplet cross sections.

Energy	15.6 eV	17.6 eV	19.6 eV	25 eV	30 eV	54.4 eV
Singlet	0.93	1.78	2.45	3.54	3.97	3.94
Triplet	0.17	0.35	0.51	0.86	1.09	1.64
Total	0.36	0.71	0.99	1.53	1.81	2.21
Asymmetry	0.52	0.51	0.49	0.44	0.40	0.26

In Table I we list the integrated ionization cross sections. The estimated accuracy of these results is the same as for the corresponding SDCS's. We should note that the SDCS's shown in Fig. 1 were normalized so that integrating over half of the energy range gives the integrated cross sections. The values for the singlet and triplet cross sections σ_S and σ_T given in Table I do not include spin statistical weights, so the total ionization cross section is $(\sigma_S+3\sigma_T)/4$. The spin asymmetry is defined as $(\sigma_S-\sigma_T)/(\sigma_S+3\sigma_T)$. For 54.4 eV collision energy the cross sections include estimates for the $L>13$ components that account for about 3% of the total.

Unlike the SDCS, the TDCS requires a construction of the complete ionization amplitude according to Eq. (2.13), so that any phase inconsistencies among the $f^L_{l_1 l_2}$ would adversely affect the calculated TDCS. In other words, the SDCS tests only the magnitudes of the calculated $f^L_{l_1 l_2}$ but the TDCS also tests the phases. In Figs. 2–7 we present the equal-energy sharing TDCS at 30, 25, 19.6, 17.6, and 15.6 eV collision energies for a variety of coplanar geometries. In these geometries the trajectories of the incident and two outgoing electrons all lie in a single plane. For instance, each panel in Fig. 2 shows a one-dimensional slice of the TDCS for 30 eV collision energy corresponding to a particular fixed angular separation θ_{12} between the directions of the two outgoing electrons.

Figure 2 contains our previous results, based on flux extrapolation, along with the current results. The agreement between the TDCS results obtained from these two very different methods is a strong indicator of the correctness of both methods. We also show this same comparison at 25 eV and 19.6 eV collision energies in Figs. 3 and 4, respectively, and found that the agreement is equally good in these cases. For the flux-extrapolation method this implies that the error introduced by extrapolating from finite box sizes was small. For our calculation of the ionization amplitude this implies that there is no phase inconsistency among the $f^L_{l_1 l_2}$ calculated at a finite hyperradius. Thus, we have found that Eq. (2.7) [or, equivalently, Eq. (2.9)] leads to a viable method of calculating the complete ionization amplitude despite the existence of a formally divergent phase.

Experimental values due to Röder *et al.* [11] are also shown in Figs. 2, 3, and 4. These results were originally

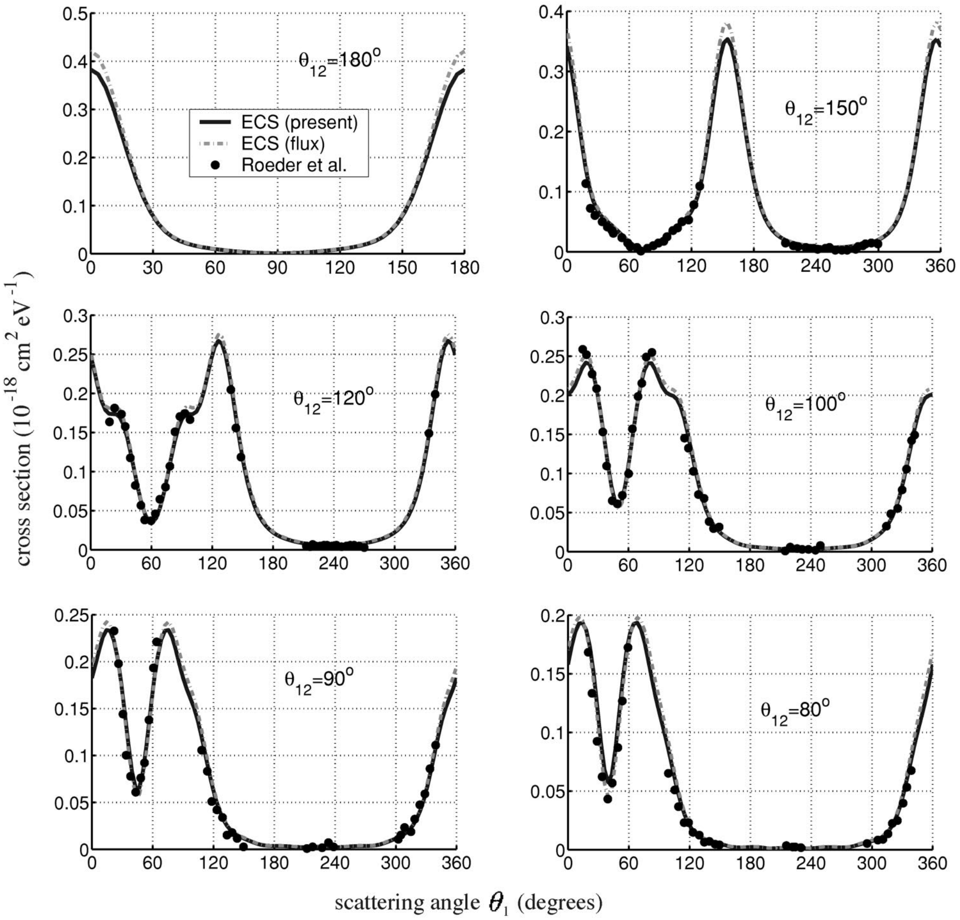

FIG. 2. Equal-energy sharing, coplanar TDCS for 30 eV incident energy with θ_{12} fixed. Internormalized measurements [11], originally reported in arbitrary units, were multiplied by 0.16 to fit calculated cross section. Solid curves: present results. Dashed curves: earlier results from Ref. [8].

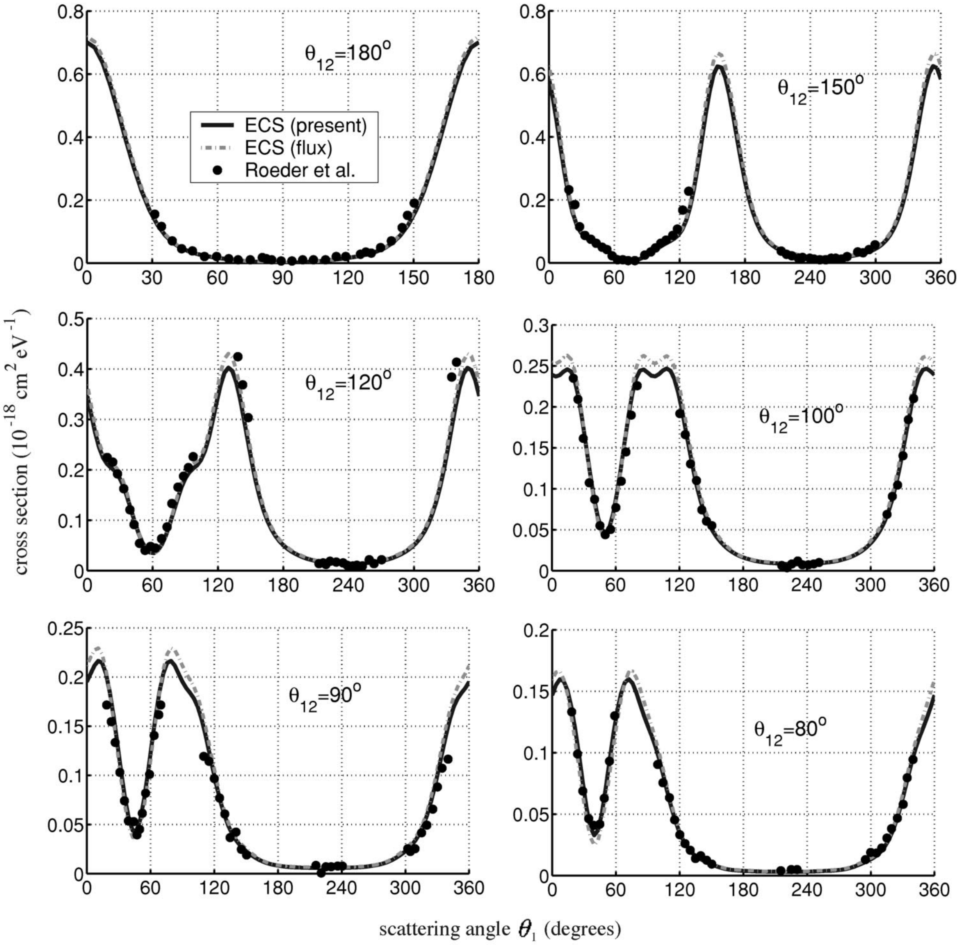

FIG. 3. Same as Fig. 2 but for 25 eV incident energy. The normalization factor to convert measured values from arbitrary units is 0.16.

presented in arbitrary units. We have normalized these values by choosing a single scaling factor to give the best overall fit between experiment and our calculations. Although comparison in absolute magnitude is not possible at these energies, we see that agreement in the overall shape is quite good. At 17.6 eV collision energy, however, we can compare with absolute experimental measurements, shown in Fig. 5. The set of fixed θ_{12} data was originally presented in arbitrary, but internormalized, units [11]. Later, the $\theta_{12}=180°$ data were remeasured in absolute units, allowing the entire set of data to be put on an absolute scale [12]. These absolute experimental data are shown, along with our TDCS results calculated using Eq. (3.1) and our earlier results based on flux extrapolation, in Fig. 5.

Agreement between our calculations and the experimental results is quite good with our results being well within the reported 40% error bars of most of the measured values. Overall, the comparison suggests that a slight reduction in the overall magnitude of the data would produce better agreement. At 17.6 eV the difference between our present results and our earlier ones derived from flux extrapolation is slightly more than at 25 eV. This is because of the greater box-size dependence at lower energies, which is more problematic for the flux-extrapolation procedure than it is for calculating the amplitudes.

In Fig. 6 we show results for two geometries at 17.6 eV where the position of one detector is held fixed at some angle θ_2. In Ref. [11] the experimental data for these geometries were normalized to fit distorted-wave Born approximation (DWBA) calculations of Whelan *et al.* and were not reported in the same arbitrary units as the fixed θ_{12} geometries. We present these experimental data as normalized by the DWBA calculations. Experimentally normalized data for these geometries do exist but have been shown by Bray to be inconsistent with the data for fixed θ_{12} [21]. Clearly, there is an internormalization issue between the fixed θ_{12} data and the fixed θ_2 data at this energy. Consequently, we prefer to present the two different classes of geometries at this energy using separate normalizations.

Finally, in Fig. 7 we show results for the TDCS at 15.6 eV collision energy. At this energy we were unable to produce reliable results using flux extrapolation. The ionization amplitude expression is less sensitive to the box size and it allows us to calculate cross sections at lower collision energies than what we were able to treat using flux extrapolation. Still, our results at 15.6 eV are somewhat less accurate, within 10% for $\theta_{12}=180°$ and perhaps more for smaller θ_{12}, than at higher energies. Absolute measurements at this energy [11,12] are available. However, Bray has suggested, based on convergent close-coupling calculations, that the normalization of the 15.6 eV data is incorrect [21]. Our calculations indicate that the absolute measurements are too high by a factor of 2. Multiplying the experimental values by

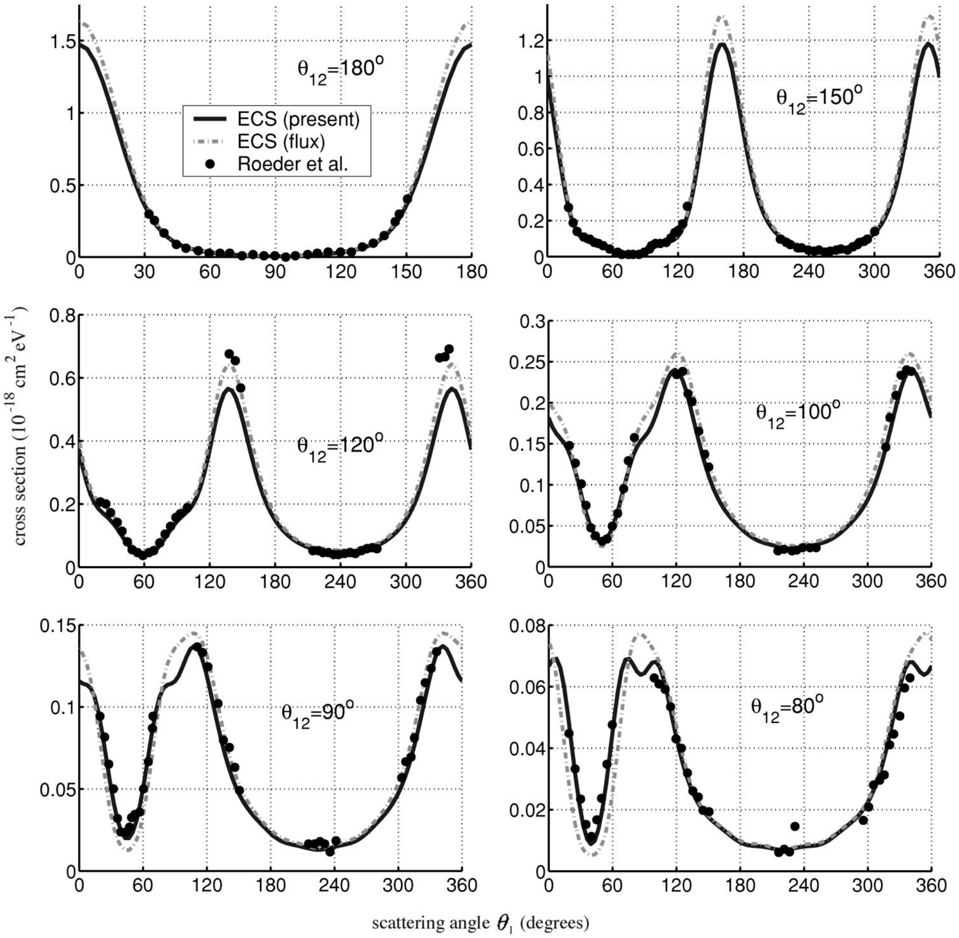

FIG. 4. Same as Fig. 2 but for 19.6 eV incident energy. The normalization factor to convert measured values from arbitrary units is 0.20.

0.5 gives good overall agreement with our results, as shown in Fig. 7. Distorted partial-wave (DPW) calculations for $\theta_{12}=180°$ by Pan and Starace [12,22] also indicate that the 15.6 eV data are too large by a factor of 2. In general, we have found that agreement between our results and DPW results (the latter available only for $\theta_{12}=180°$) is excellent. We show results for a variety of different geometries in Fig. 7. In all geometries, including those with θ_2 fixed, dividing the experimental values by two gives good agreement with our calculation. There appears to be no problem at 15.6 eV with internormalization between the fixed θ_{12} data and the fixed θ_2 data as there was at 17.6 eV.

V. DISCUSSION

We have presented a formalism for calculating the complete amplitude for electron-impact ionization and successfully applied it to electron-hydrogen scattering using a partial-wave expansion. Cross sections produced by the methods described here are more accurate than our previous results obtained by extrapolating the quantum mechanical flux. The improved accuracy is due to the new formalism being less dependent on the finite range of the calculation and being able to formally distinguish between ionization and excitation channels. The latter characteristic allows us to calculate *ab initio* differential cross sections over the entire range of energy sharing.

Although the formalism presented here offers significant improvement over our flux-extrapolation method it also serves to validate the fundamental correctness of that earlier approach. Our results are in excellent agreement with those of the DWBA and DPW methods at the limited geometries for which they are available. The shapes of our calculated SDCS agree well with semiclassical predictions [13]. They also exhibit the proper symmetry and are free from the unphysical oscillations that characterize some other *ab initio* approaches [23]. To the extent that we are able to compare with experiment, agreement is good. Agreement with experiment in the overall shape of the TDCS is very good, with the noted exception of the inconsistencies between the fixed θ_{12} and fixed θ_2 data at 17.6 eV. Absolute agreement with experiment is reasonable at 17.6 eV, but not at 15.6 eV where our calculations, as well as the work of others [12,21,22], suggest there is factor of 2 error in the normalization of the experimental data.

The rearrangement formalism presented here allows calculation of the complete ionization amplitude over a broad range of energies. In contrast to the quantum mechanical flux, whose asymptotic value generally requires calculations well beyond the range of the interaction potentials [15], the expressions we use for the ionization amplitude depend only on the range of the two-body interaction potentials and are therefore far less sensitive to the restrictions imposed by

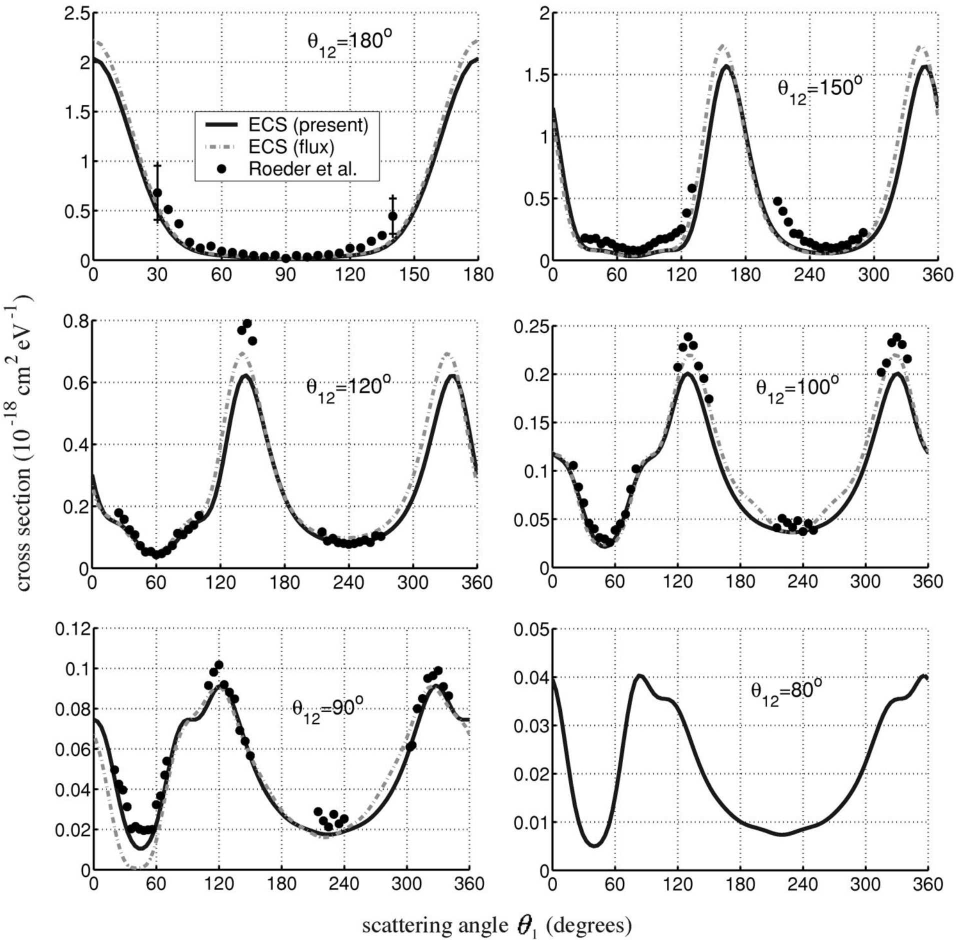

FIG. 5. Equal-energy sharing, coplanar TDCS for 17.6 eV incident energy with θ_{12} fixed. Experimental data are absolute measurements [11,12] with 40% error bars. Solid curves: present results. Dashed curves: earlier results from Ref. [8].

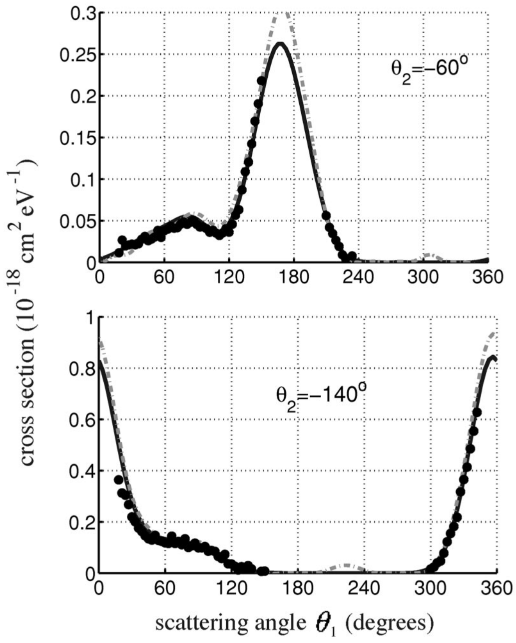

FIG. 6. Equal-energy sharing, coplanar TDCS for 17.6 eV incident energy with θ_2 fixed. Experimental data were normalized to fit calculations by Whelan *et al.* [11]. Solid curves: present results. Dashed curves: earlier results from Ref. [8].

working in a finite volume. Nevertheless, the method is not without its limitations. There are still practical lower limits to the collision energies that can be treated, since the error in the computed amplitude will scale roughly inversely with the ratio of the total energy to the value of the potential on the hypersphere used in the evaluation. With the present technology, it is currently not possible because of computational limitations to perform calculations below about 1 eV total energy. For the calculations at 15.6 eV incident energy (2 eV total energy), the surface integrals in Eq. (2.14) had to be evaluated at hyperradii in excess of $100a_0$. The minimum hyperradii will increase as the collision energy approaches threshold.

Although there is a lower limit on the collision energy, we have not noticed any limits on the energy of an outgoing electron and we believe the formalism is capable of producing accurate amplitudes even when the energy of one electron is very close to either zero or E. At higher collision energies the box-size requirements relax, but the number of terms needed in the angular momentum expansion increases. Collision energies above about 30 eV require more partial-wave terms than one would generally consider practical in an *ab initio* calculation. Thus, it is worth investigating whether some sort of perturbative approximation to the $f^{L}_{l_1 l_2}$ can be used for high L. Finally, we wish to point out that the rearrangement formalism is in no way connected to our exterior

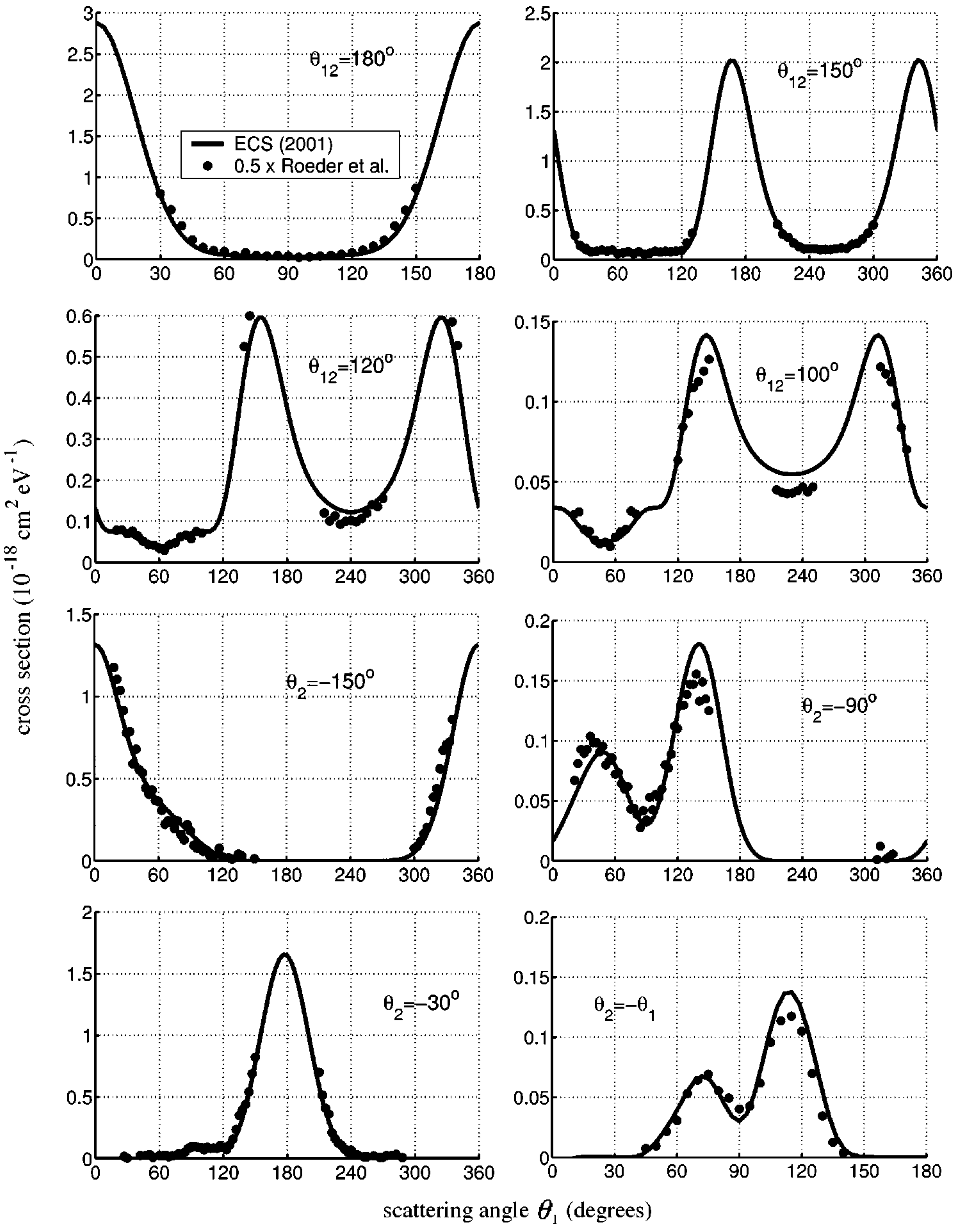

FIG. 7. Equal-energy sharing TDCS at 15.6 eV incident energy for various coplanar geometries. Absolute experimental data [11,12] have been multiplied by 0.5.

complex scaling approach to solving the Schrödinger equation. It should be readily applicable to any method that can produce a converged scattered wave at sufficiently large distances.

ACKNOWLEDGMENTS

We wish to thank Igor Bray for providing us with numerical values for the absolute experimental data at 15.6 and 17.6 eV. This work was performed under the auspices of the U.S. Department of Energy (DOE) by the University of California Lawrence Berkeley and Lawrence Livermore National Laboratories under Contract Nos. DE-AC03-76SF00098 and W-7405-Eng-48, respectively. Computational work was carried out at the National Energy Research Scientific Computing Center at Lawrence Berkeley National Laboratory. This work was supported by the Office of Energy Research, Office of Basic Energy Sciences, Division of Chemical Sciences of the U.S. DOE.

---

[1] R. K. Peterkop, Opt. Spectrosc. **13**, 87 (1962).
[2] M. R. H. Rudge and M. J. Seaton, Proc. R. Soc. London, Ser. A **283**, 262 (1965).
[3] M. R. H. Rudge, Rev. Mod. Phys. **40**, 564 (1968).
[4] H. R. Sadeghpour, J. L. Bohn, M. J. Cavagnero, B. D. Esry, I. I. Fabrikant, J. H. Macek, and A. R. Rau, J. Phys. B **33**, R93 (2000).
[5] C. W. McCurdy, T. N. Rescigno, and D. A. Byrum, Phys. Rev. A **56**, 1958 (1997).
[6] C. W. McCurdy and T. N. Rescigno, Phys. Rev. A **56**, R4369 (1997).
[7] T. N. Rescigno, M. Baertschy, W. A. Isaacs, and C. W. Mc-

Curdy, Science **286**, 2474 (1999).

[8] M. Baertschy, T. N. Rescigno, W. A. Isaacs, X. Li, and C. W. McCurdy, Phys. Rev. A **63**, 022712 (2001).

[9] W. A. Isaacs, M. Baertschy, C. W. McCurdy, and T. N. Rescigno, Phys. Rev. A **63**, 030704R (2001).

[10] M. Baertschy, T. N. Rescigno, W. A. Isaacs, and C. W. McCurdy, Phys. Rev. A **60**, R13 (1999).

[11] J. Röder, J. Rasch, K. Jung, C. T. Whelan, H. Ehrhardt, R. Allan, and H. Walters, Phys. Rev. A **53**, 225 (1996).

[12] J. Röder, H. Ehrhardt, C. Pan, A. F. Starace, I. Bray, and D. Fursa, Phys. Rev. Lett. **79**, 1666 (1997).

[13] J. M. Rost, Phys. Rev. Lett. **72**, 1998 (1994).

[14] M. D. Baertschy, Ph.D. thesis, U.C. Davis, 2000.

[15] C. W. McCurdy and T. N. Rescigno, Phys. Rev. A **62**, 032712 (2000).

[16] C. W. McCurdy, D. A. Horner, and T. N. Rescigno, Phys. Rev. A **63**, 022711 (2001).

[17] M. Baertschy, T. N. Rescigno, C. W. McCurdy, J. Colgan, and M. S. Pindzola, Phys. Rev. A **63**, 050701R (2001).

[18] C. T. Whelan, H. R. J. Walters, J. Hansen, and R. M. Dreizler, Aust. J. Phys. **44**, 39 (1991).

[19] S. P. Lucey, J. Rasch, and C. T. Whelan, Proc. R. Soc. London, Ser. A **455**, 349 (1999).

[20] R. K. Peterkop, *Theory of Ionization of Atoms by Electron Impact* (Colorado Associated University Press, Boulder, CO, 1977).

[21] I. Bray, J. Phys. B **33**, (2000).

[22] C. Pan and A. F. Starace, Phys. Rev. A **45**, 4588 (1992).

[23] I. Bray, Phys. Rev. Lett. **78**, 4721 (1997).